Available online at www.sciencedirect.com
SCIENCE DIRECT®

Journal of the European Ceramic Society 24 (2004) 1953–1956

www.elsevier.com/locate/jeurceramsoc

Intense visible light emission from three-dimensional periodical arrays of Si clusters

S. Sato*, N. Yamamoto, K. Nakanishi, H. Yao, K. Kimura

Department of Material Science, Himeji Institute of Technology, 3-2-1, Koto, Kamigori-cho, Ako-gun, Hyogo 678-1297, Japan

Abstract

We report a strong visible light photoluminescence (PL) from three-dimensional Si cluster arrays. Using a chemical self-assembly process of Si clusters in aqueous solutions, three types of array structures are prepared: (I) BCC arrays with $a=6.1$ angstroms, (II) FCC arrays with $a=7.5$ angstroms, and (III) BCC arrays with $a=6.9$ angstroms. The distance between the centers of adjacent Si clusters is 5.3 angstroms for both sample I and II, and 6.0 angstroms for the sample III. In the PL measurements, red, orange, and blue-green are the three different colors observed at peak wavelengths of 700, 610, and 530 nm, respectively. The red, orange, and blue-green light emissions are thought to originate from the samples I, II, and III, respectively. PL is strong enough to be seen by the naked eye in all the samples. Possible mechanisms for the strong visible light luminescence are discussed.

Keywords: Optical microscopy; Spectroscopy; Suspensions

1. Introduction

New materials can be engineered from existing materials that have new band structures induced by nanometer-scaled periodicity. One such material with the potential to design internal periodicity is a three-dimensional (3D) periodical array of nanoparticles or clusters.[1–3] In the past decade, a variety of 3D arrays of nanocrystals (e.g. Au,[4–6] Ag,[7,8] CdSe[1,9] etc.) and clusters (e.g. C_{60}[10] and proteins[11]) have been successfully synthesized using self-assembly processes in solution or at the surface. It has been experimentally confirmed that 3D arrays show interesting optical properties. For instance, dielectric-like optical properties can be obtained by arranging Au nanoparticles into 3D arrays;[12] optical properties of CdSe nanoparticle arrays can be systematically altered by controlling the component particle size.[2]

Recently, we have discovered that upon inverting the Si cluster surfaces from hydrophilic to hydrophobic, Si clusters spontaneously self-assemble into 3D periodic arrays at an air/aqueous solution interface[13] or at an aqueous solution/Si substrate interface.[14] In this study, we prepared three different Si cluster arrays, and evaluated their photoluminescence (PL).

2. Experimental

Si cluster arrays were fabricated using a similar method described in detail elsewhere.[13] As starting material, Si oxide particles containing a number of Si clusters were prepared by evaporating high-purity Si powders in a helium atmosphere containing approximately 0.1% air. The total pressure in the chamber was kept constant at 1 Torr. Following immersion of the Si oxide particles in distilled water, a small amount of hydrofluoric (HF) acid was added to the aqueous solution. The oxide dissolved and Si clusters were dispersed throughout the solution. Upon removing the oxide, the Si cluster surfaces were inverted from hydrophilic to hydrophobic and the Si clusters spontaneously assembled onto a hydrophobic medium (air or hydrogen-terminated Si (100) in the present experiment). The hydrogen-terminated Si substrate was prepared by immersion into a 46% HF solution. To assemble the clusters on the Si (100) surface, the Si substrate was placed on the surface of the aqueous solution. BCC arrays with $a=6.1$ angstroms, FCC arrays with $a=7.5$ angstroms, and BCC arrays with $a=6.9$ angstroms were the three types of array structures obtained. In this paper FCC arrays

* Corresponding author. Tel.: +81-791-58-0161; fax: +81-791-58-0161.
E-mail address: sato@sci.himeji-tech.ac.jp (S. Sato).

0955-2219/$ - see front matter © 2003 Elsevier Ltd. All rights reserved.
doi:10.1016/S0955-2219(03)00522-3

with $a = 7.5$ angstroms, BCC arrays with $a = 6.1$ angstroms, and BCC arrays with $a = 6.9$ angstroms will be abbreviated to FC-7.5, BC-6.1 and BC-6.9, respectively.

The morphologies and the packing structures of the arrays were examined with a transmission electron microscope (TEM: Hitachi H-8100) operated at 200 kV. PL measurements were conducted at room temperature using the 435 nm line of a mercury lamp with an optical bandpass filter as an excitation source.

3. Results and discussion

Fig. 1 shows typical TEM images and transmission electron diffraction (TED) patterns of the Si cluster arrays grown at an air/solution interface. From our previous TEM and TED studies,[13] the following structural information has been revealed. The packing arrangements in the arrays grown at an air/solution interface are either FC-7.5 or BC-6.9. The BC-6.9 arrays tend to be larger than the FC-7.5 arrays, but the FC-7.5 arrays tend to form well-resolved facets while the BC-6.9 arrays form obscure faces. Typical widths are between 1 and 10 μm for BC-6.9 and between 0.1 and 3 μm for FC-7.5. Typical morphological differences can be seen by comparing Fig. 1 (a) and (b). BC-6.1 and BC-6.9 are grown on the Si substrate.[14] Both arrays measure ~1 μm and characteristic differences in morphology are not found. Since the distances to the nearest neighbor between lattice points in BC-6.1 and FC-7.5 are equivalent, the component clusters are thought to be identical.

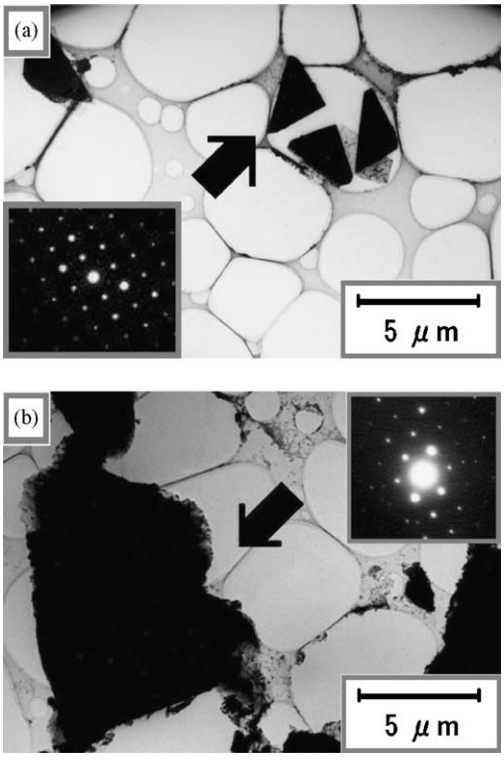

Fig. 1. Typical TEM images of the cluster arrays grown at an air/solution interface: (a) FC-7.5 and (b) BC-6.9. The insets are the TED patterns of the samples indicated by the arrow. The samples are placed on a specimen grid covered with a perforated carbon film.

The Si cluster arrays show intense PL in the visible region. The starting material, the Si oxide containing the Si clusters, and the Si clusters dispersed in the HF solution showed no detectable luminescence in the range of 450–950 nm. Fig. 2 shows the PL image and the spectra of the samples grown at an air/solution interface. Blue-green and orange are the two PL colors observed with peak wavelengths of 530 and 610 nm, respectively. After analyzing numerous PL images, we found that the blue-green PL tended to have a larger emission area than the PL of orange, especially when the sample was greater than ~4 μm.

Fig. 3 shows the PL results of the samples grown at a solution/Si substrate interface. Two colors, blue-green and red, are displayed in the PL images and the peak energies are 530 and 700 nm, respectively. The blue-green PL in Fig. 3 is identical to that in Fig. 2.

Therefore, the data are consistent with the following conclusions. BC-6.9 emits the blue-green PL because of the following two findings. First, only BC-6.9 and FC-7.5 are found in samples grown at the air/solution interface and FC-7.5 crystals typically do not grow as large as ~4 μm. Second, BC-6.9 is the only array found in samples grown at both the air/solution and the solution/Si substrate interfaces. The orange PL originates from FC-7.5 since it is the only other structure formed at the air/solution interface, while the red PL is derived from BC-6.1.

Four plausible mechanisms for the PL are considered below. The first mechanism is an interband recombination in newly created band structures. As previously mentioned, the TED studies indicate three unique packing structures. The differences in packing structures cause three types of bandgap energies, which may result in the various PL colors. The second possible mechanism is the recombination via radiative centers originating in Si/H/O molecules adsorbed at the surface of the arrays. For instance, PL peak wavelength of siloxene ($Si_6O_3H_6$) continuously shifts between 500 and 800 nm after annealing.[15] Assuming that different Si/H/O compounds grow on the surfaces of different array structures, it is possible that three types of PL can be observed. The third possibility is that the variations in PL color may arise from defect centers grown in the different arrays.

If the origin of PL is from Si/O/H molecules or defects, then it may be argued that PL is not necessarily dependent on the array structure. The following experimental results, however, indicate that structural dependence should be incorporated into PL mechanism. First, all the samples that are grown at the air/solution

interface larger than ~4 μm emit blue-green PL. This implies that BC-6.9 is the sole source of blue-green PL since FC-7.5 does not grow that large. Second, orange PL is only observed in samples grown at an air/solution interface while red is only seen in samples grown at a solution/Si substrate interface. This is consistent with the TED results that BC-6.1 is not found at an air/solution interface, and FC-7.5 is not found at a solution/Si substrate interface. Therefore, it is reasonable to speculate that the PL color is related to the array structure.

The fourth and more plausible mechanism is a combination of the above mechanisms, which would be analogous to the discussion of strong visible PL from Si nanostructures such as porous Si and Si nanoparticles. The following often explains PL from Si nanostructures.[16–19] Absorption occurs at Si nanocrystals and the excited electron-hole pairs recombine via radiative centers originating in surface Si/O/H molecules or defects at the surface. The bandgap of Si nanostructures is widened due to the carrier confinement, which may facilitate an efficient supply of carriers into the radiative centers at the surface. For Si cluster arrays, the newly created bandgaps may play a similar role to the widened bandgaps in Si nanostructures. Extensive studies are needed to clarify the PL mechanism of Si cluster arrays. These studies are currently underway and include low temperature optical absorption experiments, electronic structure evaluations using photoelectron spectroscopy or scanning tunneling spectroscopy, and the identification of Si/O/H compounds at the surface of the arrays.

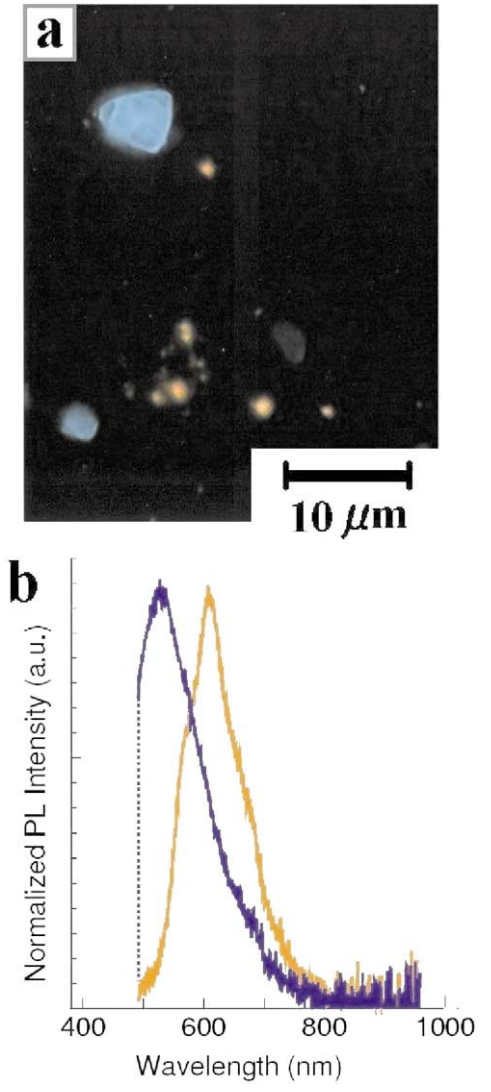

Fig. 2. PL from Si cluster arrays grown at an air/solution interface: (a) the optical micrograph; and (b) the PL spectra of the blue-green and orange light emitting samples. The steep decrease (dotted line) is due to use of an optical cut-off filter of 480 nm to keep excitation light from entering the detector.

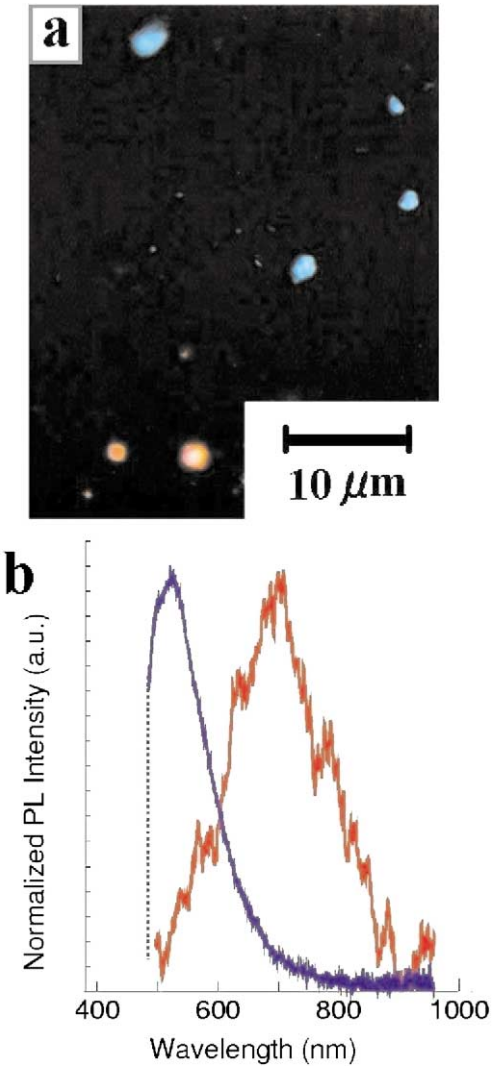

Fig. 3. PL from Si cluster arrays grown at a solution/Si substrate interface: (a) the optical micrograph; and (b) the PL spectra of the blue-green and red light emitting samples. The steep decrease (dotted line) is due to use of an optical cut-off filter of 480 nm to keep excitation light from entering the detector.

4. Summary

Intense blue-green, orange, and red light emissions were observed from Si cluster arrays with peak energies in the PL spectra of 530, 610 and 700 nm, respectively. All three types of PL were strong enough to be seen by the naked eye. By comparing characteristic features of the arrays seen in PL images and those in TEM images, blue-green, orange, and red PL were concluded to be from BC-6.9, FC-7.5 and BC-6.1, respectively. The observed PL was similar to that from Si quantum dots/wires although carriers are not confined in the present systems. It is feasible that the newly created bandgaps in the cluster arrays play an important role as to the intense visible light emission. Although possible PL mechanisms were discussed, extensive studies, which are currently underway, are needed to justify them.

Acknowledgements

The Nippon Sheet Glass Foundation for Materials Science and Engineering supported this study.

References

1. Collier, C. P., Vossmeyer, T. and Heath, J. R., Nanocrystal superlattices. *Annu. Rev. Phys. Chem.*, 1998, **49**, 371–404.
2. Murray, C. B., Kagan, C. R. and Bawendi, M. G., Synthesis and characterization of monodisperse nanocrystals and close-packed nanocrystals assemblies. *Annu. Rev. Mater. Sci.*, 2000, **30**, 545–610.
3. Saito, S. and Oshiyama, A., Cohesive mechanism and energy bands of solid C_{60}. *Phys. Rev. Lett.*, 1991, **66**, 2637–2640.
4. Whetten, R. L., Shafigullin, M. N., Khoury, J. T., Schaaff, T. G., Vezmar, I., Alvarez, M. M. and Wilkinson, A., Crystal structures of molecular gold nanocrystals arrays. *Acc. Chem. Res.*, 1999, **32**, 397–406.
5. Kimura, K., Sato, S. and Yao, H., Particle crystals of surface modified gold nanoparticles grown from water. *Chem. Lett.*, 2001, 372–373.
6. Sato, S., Yamamoto, N., Yao, H. and Kimura, K., Substrate dependence in the growth of three-dimensional gold nanoparticle superlattices. *Mat. Res. Soc. Symp. Proc.*, 2002, **703**, 375–380.
7. Harfenist, S. A., Wang, Z. L., Alvarez, M. M., Vezmar, I. and Whetten, R. L., Highly oriented molecular Ag nanocrystals arrays. *J. Phys. Chem.*, 1996, **100**, 13904–13910.
8. Taleb, A., Petit, C. and Pileni, M. P., Synthesis of highly monodisperse silver nanoparticles from AOT reverse micelles: a way to 2D and 3D self-organization. *Chem. Mater.*, 1997, **9**, 950–959.
9. Murray, C. B., Kagan, C. R. and Bawendi, M. G., Self-organization of CdSe nanocrystallites into three-dimensional quantum dot superlattices. *Science*, 1995, **207**, 1335–1338.
10. Krätschmer, W., Lamb, L. D., Fostiropoulos, K. and Huffman, D. R., Solid C_{60}: a new form of carbon. *Nature*, 1990, **347**, 354–357.
11. McPherson, A., *Crystallization of Biological Macromolecules*. Cold Spring Harbor Laboratory Press, New York, 1999.
12. Sato, S., Yao, H. and Kimura, K., Optical absorption properties of three-dimensional Au nanoparticle crystals. *Chem. Lett.*, 2002, 526–527.
13. Sato, S., Yamamoto, N., Yao, H. and Kimura, K., Synthesis of three-dimensional silicon cluster superlattices. *Chem. Phys. Lett.*, 2002, **365**, 421–426.
14. Sato, S., Yamamoto, N., Nakanishi, K., Yao, H. and Kimura, K., Three-dimensional arrays of Si clusters grown at water surfaces and Si (100) surfaces. *Microelectronic Eng.*, 2003, **66**, 159–165.
15. Fuchs, H. D., Stutzmann, M., Brandt, M. S., Rosenbauer, M., Weber, J., Breitschwerdt, A., Deak, P. and Cardona, M., Porous silicon and siloxene: vibrational and structural properties. *Phys. Rev. B*, 1993, **48**, 8172–8189.
16. Murayama, K., Miyazaki, S. and Hirose, M., Visible photoluminescence from porous silicon. *Jpn. J. Appl. Phys.*, 1992, **31**, L1358–L1361.
17. Qin, G. G. and Jia, Y. Q., Mechanism of the visible luminescence in porous silicon. *Solid State Commun.*, 1993, **86**, 559–563.
18. Cooke, D. W., Bennett, B. L., Farnum, E. H., Hults, W. L., Sickafus, K. E., Smith, J. F., Smith, J. L., Taylor, T. N., Tiwari, P. and Portis, A. M., SiOx luminescence from light-emitting porous silicon: support for the quantum confinement/luminescence center model. *Appl. Phys. Lett.*, 1996, **68**, 1663–1665.
19. Sato, K., Sugiyama, Y., Izumi, T., Iwase, M., Show, Y., Nozaki, S. and Morisaki, H., *Mat. Res. Soc. Symp. Proc.*, 1998, **536**, 57–62.